Linear Analysis of Vortex-Shedding Induced Longitudinal Oscillations in Segmented Solid Rocket Motors

(Analisi Lineare di Oscillazioni Longitudinali in Razzi a Solido Segmentati Indotte dal Distacco di Vortici)

Ciucci A.[1], d'Auria F.[2] and d'Agostino L.[3]

CENTROSPAZIO, Pisa

Abstract

A linear model for the analysis of longitudinal fluid dynamic oscillations in solid rocket motors is developed and applied to the Ariane 5 boosters. The natural frequencies are corrected as proposed by Culick in order to account for the effects of mean flow, mass addition from the burning grain, pressure coupling, nozzle admittance, and internal geometry of the combustion chamber. In segmented solid rocket motors, the main driving source of acoustic oscillations is often represented by the coupling between the vortices shed by the inhibitors at the intersegments and the acoustic field in the combustion chamber. This interaction is analyzed using Flandro's model, which provides the vortex-related contribution to the amplification/damping of the acoustic oscillations. The natural acoustic frequencies are considered as known inputs for vortex development in the shear layer, which is described by means of classical linear stability theory of parallel flows. The risk assessment of vortex-induced fluid dynamic instabilities in a small scale and full size configuration of the Ariane 5 boosters is carried out for the leading modes at several burn times. Model predictions are in good agreement with the available experimental results for the scaled configuration.

1. Introduction

Fluid dynamic oscillations in combustion chambers represent today one of the most stringent limitations to rocket motor performance, since they often are responsible for very serious problems, ranging from the development of unacceptable pressure/thrust fluctuations to the occurrence of irreversible destructive damage to the motor. In general, fluid dynamic oscillations can sustain themselves through energy coupling with either the combustion process itself, or the propellant mean flow. In both cases, but especially in the first one, even relatively inefficient coupling mechanisms can be sufficient to produce significant damage, given the high energy released by propellant combustion, or associated with its flow through the chamber. In solid propellant rockets, the coupling with the combustion process is usually determined by the response of the burning rate to pressure and/or velocity perturbations. This effect is further complicated by the influence of the oscillation frequency, and, at least in linearized theories, is usually accounted for by means of suitably defined admittance functions. On the other hand, global fluid dynamic oscillations in the combustion chamber can also be sustained by the occurrence of local instabilities of the mean flow capable of interfering with the rest of the flow field. Typical in this respect and quite important in practice are the unsteady vortical layers originating from the inhibitors in segmented solid rocket motors, as they gradually protrude in the mean flow with progress of grain combustion.

A comprehensive analysis of flow instabilities in a combustion chamber, although desirable in principle, is limited by the remarkable difficulties in developing a representative model, due to the complexity of the physical phenomena involved. The stability of fluid dynamic oscillations in combustion chambers is a major aspect of rocket design, and has therefore received considerable attention in recent years (Culick 1970, 1973, 1975, 1990; Yang *et al.*, 1990; Kuentzmann, 1991). In this respect, linearized models are quite adequate, and represent an attractive trade-off between simplicity and generality. On the other hand, the linear nature of these models clearly precludes their application to the study of the development of the oscillations beyond the linear range. Given the practical difficulties and high costs of fire tests, there is a great need for validation of theoretical models for prediction of rocket flow stability ranges.

In the present work, the linear stability problem of the fluid dynamic oscillations induced by the vortical wakes generated by the inhibitors in segmented solid rocket motors is specifically addressed. The acoustic field in the combustion chamber is described according to Culick's quasi-one-dimensional formulation (Culick 1974), including the effects of mass addition from the burning grain, mean flow in the chamber, pressure coupling, nozzle admittance, and, to some extent, internal geometry of the chamber. The classical linear stability theory of parallel shear flows is used to describe the vortical field generated by the inhibitors. The associated boundary value eigenproblem for the linear perturbation equation is solved numerically by the multiple shooting method, and the interactions between the acoustic and vortical fields are treated as suggested by Flandro, 1986. The combined model is then validated by comparison with experimental data reported in the literature (Vuillot *et al.*, 1993) relative to scaled fire tests on the Ariane 5 boosters, and finally applied to assess the risk of vortex-induced instabilities for the full-scale configuration.

2. Formulation

In the instability model proposed by Flandro, the acoustic field in the combustion chamber provides the forcing frequency for the development of the vortices shedding from the inhibitors. The determination of this frequency requires the solution of the unsteady flow field in the combustion chamber. Various levels of refinement can be adopted to this purpose. In the simplest case, the classical Helmholtz solution of the one-dimensional homogeneous wave equation in the combustion chamber can be used. However, this approach does not account for the effects of mass addition from the burning grain, mean flow velocity, pressure and velocity coupling of the combustion rate, nozzle admittance, internal geometry of the chamber, suspended solid particulates, and grain motion, which are known to be significant in practice. To a higher level of approximation, inclusion of these effects in a linearized analysis as originally suggested by Culick, 1970, leads to the solution of a non-homogeneous one-dimensional wave equation:

$$\frac{\partial^2 p'}{\partial X^2} - \frac{1}{\bar{a}^2}\frac{\partial^2 p'}{\partial t^2} = h \qquad \text{with} \qquad \frac{\partial p'}{\partial X} = -g$$

where p' is the pressure perturbation, and explicit expressions of the known terms h and g account for the above-mentioned effects. All of the flow properties of the acoustic field are normalized with respect to the following reference quantities: length L, velocity $\bar{a}$, time $L/\bar{a}$, pressure $\gamma\bar{p}$. For one-dimensional harmonic oscillations with complex frequency ω, wave number $k = \omega/\bar{a}$, and complex representation $\bar{p}(X)e^{-i\omega t}$, the linearized solution of this equation is obtained as a small perturbation of the homogeneous Helmholtz solution for the l-th mode $\bar{P}_l = \cos(K_l X)$, where $K_l = l\pi/L$. To the first order:

$$k_l^2 = K_l^2 + i\frac{2K_l}{l}\left(\overline{M}_e + A_n\right) + i\frac{K_l\overline{m}_b}{\bar{p}\bar{a}L\varepsilon} - \frac{2}{L}\int_0^L \bar{P}_l\frac{d\bar{P}_l}{dX}\frac{1}{A}\frac{dA}{dX}dX - i\frac{K_l\overline{m}_b\left(\overline{M}_b + A_b\right)}{\bar{p}\bar{a}L\varepsilon\overline{M}_b}$$

where $\overline{M}_e$ and $\overline{M}_b$ are the average Mach numbers at the combustion chamber outflow boundary and at the burning surface, A_n and A_b are the admittances of the nozzle and grain surface, $\bar{p}$ and $\bar{a}$ are the mean density and sound speed in the chamber of length L and cross-sectional area A, $\overline{m}_b$ is the mean propellant mass flow rate, and $0 \le \varepsilon \le 1$ is a numerical factor accounting for non-burning regions along the chamber. This equation determines the corrected modal frequencies ω_l required as inputs to the linear stability analysis of the vortical wake of the inhibitors. A similar expression holds for the corresponding mode shapes. In the above, all of the unperturbed flow properties in the combustion chamber are assumed uniform in space and equal to their mean values.

In the linear approximation, the dynamics of the vortical flows in the shear layers generated by the inhibitors is adequately described by the standard linear stability analyses of parallel flows. By representing the flow perturbations in complex form and assuming harmonic solutions both in time and in the streamwise x-direction, the classical Rayleigh or Orr-Sommerfeld equations are obtained for incompressible, two-dimensional, thin shear layers with self-similar unperturbed velocity profiles $U(r)$ in the transverse r-direction. For non-diverging far field solutions outside the shear layer, a characteristic problem with homogeneous boundary conditions must be solved, which allows the determination of either the complex frequency $\omega = \omega_r + i\omega_i$ or the complex wave number $\alpha = \alpha_r + i\alpha_i$ of the vortical wake. Here, for constant amplitude acoustic oscillations in the combustion chamber, the frequency is real and fixed, being equal to the modal frequency under consideration $\omega = \omega_l$. Then, the solution of the linear stability problem determines the corresponding complex wave number (spacewise stability analysis), and completely defines the dynamics of the entire vortical wake to within a multiplicative constant.

Notice that the Rayleigh equation is never singular for the problem of interest, since real group velocities ω/α correspond to marginally stable wakes, which are clearly incapable of providing effective excitation of the acoustic field in the combustion chamber. Besides, vortical wakes in separated shear layers are essentially dominated by the balance of inertial and pressure forces, while the viscosity enters the problem only indirectly through its effects on the mean velocity profile. Therefore, the Rayleigh formulation has been preferred, since the theoretical advantages of the more rigorous approach based on the Orr-Sommerfeld equation would largely be offset in practice by the additional complications associated with its higher differential order and ill-conditioned behavior at high Reynolds numbers.

All of the flow properties of the vortical layer have been normalized with respect to the following reference quantities: length δ (shear layer thickness), velocity ΔU (free stream velocity difference across the shear layer), time $\delta/\Delta U$, pressure $\overline{\rho}(\Delta U)^2$, vorticity $\Delta U/\delta$. Since δ may be comparable to the radius of the combustion chamber, the axisymmetric form of the Rayleigh equation for the complex amplitude of the radial velocity perturbation has been written in cylindrical coordinates x, r, ϑ as:

$$\bar{v}'' + \frac{\bar{v}'}{r} - \left(\frac{U'' - U'/r}{U - \omega/\alpha} + \alpha^2 + \frac{1}{r^2}\right)\bar{v} = 0$$

where primes indicate differentiation with respect to the radial coordinate r. Inside the shear layer the above equation must be integrated numerically.

The general solution for the complex amplitude of the pressure perturbation in the free stream outside the shear layer is known to be $\bar{p}(r) = C_1 I_0(\alpha r) + C_2 K_0(\alpha r)$, where $I_0(z)$ and $K_0(z)$ are the modified Bessel functions of order zero and complex argument z, with the arbitrary constants C_1 and C_2 properly chosen on each side of the shear layer in order to avoid nonphysical diverging solutions. By matching the pressure perturbation profile in the free stream to the numerical solution inside the shear layer at the points $r = R_o \pm \delta/2$ (symmetrically located with respect to the radial position R_o of the critical axis, defined as the mean flow streamline through the origin of the shear layer), the following boundary conditions:

$$\alpha\bar{v}K_0''(\alpha r) - \bar{v}'K_0'(\alpha r) = 0 \quad \text{at} \quad r = R_0 + \delta/2$$

$$\alpha\bar{v}I_0''(\alpha r) - \bar{v}'I_0'(\alpha r) = 0 \quad \text{at} \quad r = R_0 - \delta/2$$

are obtained, as required to fully define the characteristic problem for the Rayleigh equation on a bounded interval $r = R_o \pm \delta/2$. The location of the matching points is essentially arbitrary in the region outside the shear layer, and has negligible effects on the results of the stability analysis of the vortical wake. In order to make the problem determined, the eigenfunction $\bar{v}$ is normalized to unity at the initial point of the numerical integration (here $r = R_o + \delta/2$).

The eigenproblem for the complex wave number α is transformed in a standard boundary value problem by the addition of the auxiliary differential equations $\alpha_r' = 0$ and $\alpha_i' = 0$ (where primes indicate differentiation with respect to the radial coordinate), and solved numerically by a multiple shooting technique. The integration is performed by a fourth order Runge-Kutta method, with extrapolation to fifth order and adaptive step size for improved speed and efficiency. The error correction of the shooting algorithm employs a modified Newton-Raphson method (Stoer and Burlish 1976) in order to increase convergence capabilities. As a whole, the boundary value solver has been tested on standard ill-conditioned cases (Stoer and Burlish 1976), and proved very efficient even in single precision. For the present application, it has

been successfully validated against known results of both timewise and spacewise stability analyses (Betchov and Criminale 1967, Michalke 1965). The computed eigenfunctions are reported in Figures 1, 2 and 3 for comparison; the eigenvalues fully agree with the reference results to all available digits. The solution of the typical characteristic problem in the present work requires about 30 to 40 s on a PC/486-50MHz for convergence to a relative error better than 10^{-6}.

According to Culick, 1966, and Flandro, 1986, the interactions between the shear layer and the acoustic field in the combustion chamber arise as a consequence of the acoustic pressure emission of the vortical flow. This emission, in turn, comprises two distinct components: a quadrupole contribution due to the convective motion of the vortices, and a dipole acoustic pressure generation consequent to the interaction of the vortices with a downstream boundary S, this latter contribution being dominant. In Flandro's original formulation, the vortices are supposed to impinge on a solid surface (usually the convergent portion of the nozzle), where the satisfaction of the velocity boundary condition for impermeable walls requires an acoustic pressure to be generated (reflected wave). The same phenomenon also occurs when the unsteady vortical wake passes through the sonic section of the nozzle, which is characterized by a very low acoustic admittance. This is actually the case in the present situation, where the critical axis of the shear layer coincides, by definition, with the average streamline dividing the propellant flows originating from the burning grain located upstream and downstream of the inhibitor.
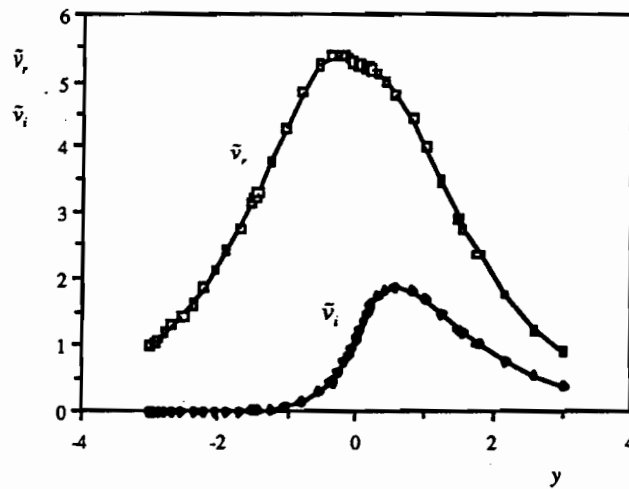

Figure 1. Complex amplitude of the y-velocity component $\tilde{v}$ v/s the transversal coordinate y in a 2-D shear layer with $U/\Delta U = \tanh(y/\delta)$, $\alpha = 0.8$ (timewise analysis).
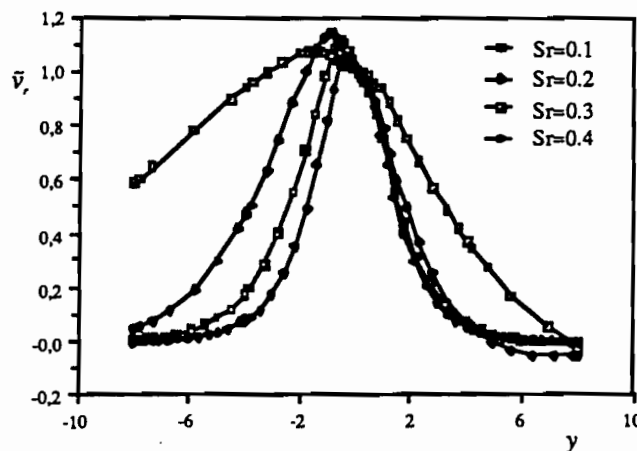

Figure 2. Real part of the complex amplitude of the y-velocity component $\tilde{v}$ v/s the transversal coordinate y in a 2-D shear layer with $U/\Delta U = 0.5[1 + \tanh(y/\delta)]$, for various values of $Sr = \omega\delta/\Delta U$ (spacewise analysis).
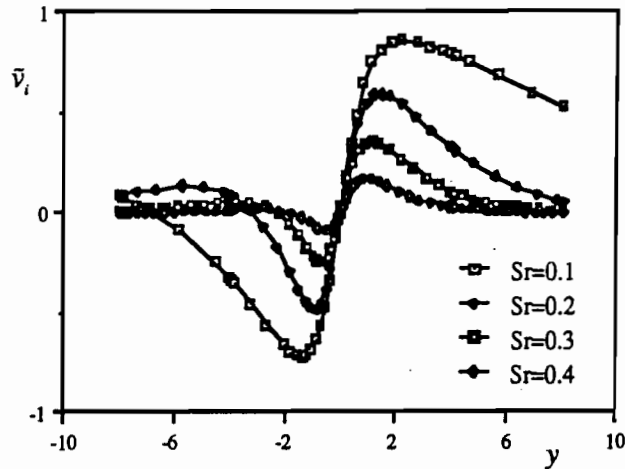
754

Figure 3. Imaginary part of the complex amplitude of the y-velocity component $\bar{v}$ v/s the transversal coordinate y in a 2-D shear layer with $U/\Delta U = 0.5\left[1+\tanh\left(y/\delta\right)\right]$, for various values of Sr $= \omega\delta/\Delta U$ (spacewise analysis).

The contribution β_v of the vortical wake to the amplification-damping rate of the oscillations in the combustion chamber as a consequence of the work done on the acoustic field is expressed by:

$$\beta_v = \frac{\overline{M}_c^2 \int_S \langle p_v' u_a' \rangle n \cdot dS}{2 \int_V \langle p'^2 \rangle dV}$$

where V is the volume of the combustion chamber, n is the unit vector in the axial direction of the flow velocity, dS is the element of the downstream boundary surface in the direction of its outward normal, $\overline{M}_c$ is the average Mach number in the combustion chamber, while p_v' and u_a' are, respectively, the (real) perturbations of vortical pressure and acoustic velocity, all quantities being normalized. Hence, the sign of the amplification/damping rate β_v of the acoustic oscillations is crucially dependent on the relative phase of p_v' and u_a' (and therefore of the vortical and acoustic fields). It is therefore necessary to uniquely characterize the development of the vortical wake by imposing the appropriate initial conditions at the shear layer origin (the inhibitor). In Flandro's model this is done by requiring that the sum of the perturbation vorticity ζ_a due the interaction of the acoustic field with the unperturbed velocity profile of the shear layer and the perturbation vorticity ζ_v of the wake be equal to zero at the inhibitor:

$$\zeta_a + C\zeta_v = 0 \qquad \text{at} \qquad x = 0 \quad \text{and} \quad r = R_0$$

since, in the absence of viscosity, the total vorticity must clearly be continuous through the shear layer origin. As a solution of a characteristic problem, ζ_v (as well as all related vortical perturbation quantities) is only known to within a proportionality factor C, which is determined by the above equation. Consistently with the linear approach, the complex acoustic velocity u_a' is approximated by the classical Helmholtz mode:

$$u_a' = -i \sin \frac{\omega X}{\overline{a}} e^{-i\omega t}$$

If, in addition, the downstream surface S is perpendicular to the rocket axis, p_v' and u_a' are constant on S, and the complex amplitude of the pressure perturbation is $\tilde{p}_v(r) \approx 1$ (as confirmed by numerical computations) then, after some tedious but relatively straightforward algebra, the linearized expression of the amplification/damping rate β_v is found to be:

$$\beta_v = \frac{\Omega}{\left|\tilde{\zeta}_v\right|}\Bigg|_{\substack{x=0 \\ r=R_0}} \frac{\overline{M}_c^2 S e^{-\alpha_i \ell}}{L} \cos\frac{\omega X_0}{\overline{a}} \sin\frac{\omega(X_0+\ell)}{\overline{a}} \sin\left(\alpha_r \ell - \arg\tilde{\zeta}_v\Big|_{x=0,\, r=R_0}\right)$$

755

Here Ω is the shear layer unperturbed vorticity, and X_0 is the axial location of the inhibitor spaced at a distance ℓ from S. Hence, β_v can be written as an explicit function of acoustic, vortical, and geometric parameters, and, in the absence of other contributions, the stability of acoustic oscillations only depends on the sign of the following coefficient:

$$C_{\beta_v} = \cos\frac{\omega X_0}{\overline{a}} \sin\frac{\omega(X_0+\ell)}{\overline{a}} \sin\left(\alpha_r\ell - \arg\bar{\zeta}_v\Big|_{x=0, r=R_o} \right)$$

Acoustic oscillations will be amplified (damped) when $1 \geq C_{\beta_v} > 0$ $(-1 \leq C_{\beta_v} < 0)$.

3. Results

The instability model has been validated by comparison with experimental data from the literature (Vuillot et al., 1993) relative to fire tests conducted by ONERA on the LP3 motor, a 1:15 scaled version of the Ariane 5 P230 rocket booster. This motor utilizes a non-metallized marginally stable propellant, potentially capable of promoting longitudinal acoustic oscillations. Finally, the present linear stability model has been employed to assess the risk of vortex-induced oscillations for the full scale configuration of the Ariane 5 P230 booster.

The internal geometry of the combustion chamber assumed for the computations is schematically illustrated in Figure 4. The relevant geometric and ballistic data are summarized in Tables 1 and 2. The analysis has been carried out for the inhibitor nearer to the chamber midpoint (here the second one), which is known to be the most critical one for the stability of longitudinal oscillations (Brown et al., 1981).

Table 1. Geometric data.

		LP3 motor	Ariane 5 booster
R_e	[m]	0.0995	1.5
R_{c1}	[m]	0.045	0.722
R_{c2}	[m]	0.045	0.722
X_1	[m]	0.233	3.38
X_o	[m]	0.908	11.43
d_1	[m]	0.002	---
d_2	[m]	0.002	---

Table 2. Ballistic data.

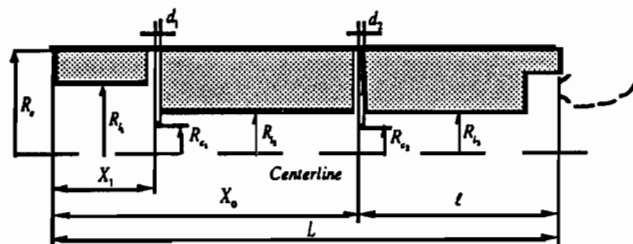|		LP3 motor	Ariane 5 booster
γ		1.2173	1.174
c_p	[J/kg·K]	1840	2010
T	[·K]	2910	3373
a	[m/s·Pa^n]	$4.1\cdot10^{-6}$	$2.628\cdot10^{-5}$
n		0.49	0.37
ρ_p	[kg/m^3]	1640	1752
c	[m/s]	1470	1574
L	[m]	1.563	23.40
$\overline{M}$		0.3	0.3
X_o	[m]	0.908	13.43
ℓ	[m]	0.722	10.11

Figure 4. Schematic of the combustion chamber geometry.

Scaled Motor

Recalling that the linear stability model has been derived under the assumption of low Mach numbers,

the reference length of the combustion chamber of the scaled LP3 motor is slightly shorter than the physical dimension, and has been taken equal to the axial location of the converging portion of the nozzle where the average Mach number is $\overline{M} = \overline{M}_c = 0.3$. Consistently with earlier considerations, the distance ℓ has been taken equal to the axial separation of the inhibitor and the nozzle throat. Since the average pressure $\overline{p}$ in the combustion chamber changes with time from ignition, the computations have actually been carried out for two representative values, $\overline{p} = 5.134$ MPa and $\overline{p} = 5.484$ MPa, corresponding to 26.6% and 75% of web combustion, respectively. The first four longitudinal acoustic modes have been investigated. The relative frequencies, corrected according to Culick's theory, are plotted in Figure 5 as a function of time from ignition. In the lack of experimental data, the mean velocity profiles of the shear layer stemming from the inhibitor had to be obtained from the steady state numerical simulations of the flow in the combustion chamber (Vuillot *et al.*, 1993).
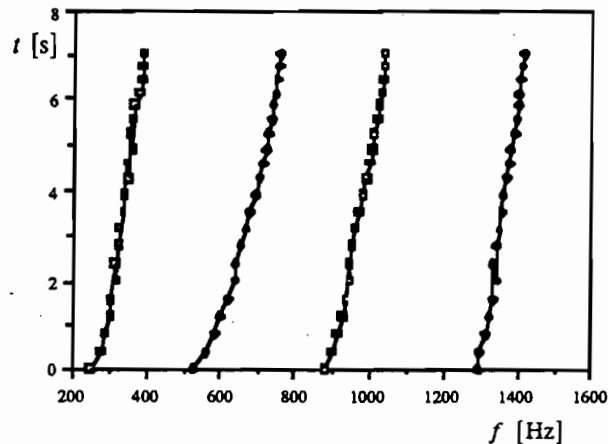

Figure 5. Corrected frequencies $f_i = \omega_i/2\pi$ for the first four longitudinal modes of the LP3 motor as a function of burn time.

Table 3. Modal frequencies and wave numbers. LP3 motor, 26.6% web combustion.

mode	f [Hz]	α_r	α_i
1L	311.6	0.085	-0.034
2L	634.5	0.156	-0.111
3L	947.8	0.224	-0.232
4L	1339.5	0.381	-0.389

Table 4. Modal frequencies and wave numbers. LP3 motor, 75.% web combustion.

mode	f [Hz]	α_r	α_i
1L	361.7	0.113	-0.057
2L	731.2	0.204	-0.192
3L	1019.1	0.326	-0.346
4L	1393.8	0.504	-0.501

Linear stability analyses of parallel flows are quite sensitive to the details of the unperturbed velocity profile of the shear layer in the proximity of the critical axis, in particular to the presence of inflection points. Therefore, the numerically simulated velocity profile must be smoothed in order to eliminate the errors due to precision limitations, which would introduce spurious inflection points in addition to the natural one on the critical axis. To this purpose, the standard fitting to an hyperbolic tangent profile in the core of the shear layer has been used. This proved to be an acceptable approximation regardless of the axial location along the chamber, thus confirming the essential validity of the self-similarity assumption (see, for example, Figure 6).

The frequencies and the corresponding wave numbers obtained from the shear layer stability analysis for the first four longitudinal modes are reported in Tables 3 and 4. An example of the dependence of the complex wave number on the acoustic frequency (Strouhal number) is also shown in Figure 7 for one burn time. Typical behaviors of the amplitude and phase of the perturbation vorticity in the shear layer of the inhibitor are plotted in Figure 8 and 9, respectively.

The results of the stability analysis of the first four longitudinal modes in the combustion chamber under the excitation provided by the vortical wake from the inhibitor are summarized in Tables 5 and 6 for the two combustion times under consideration. The corresponding experimental results, also shown in the same Tables, have been obtained from the waterfall plots reported by Vuillot *et al.*, 1993. The

interpretation of these plots is somewhat uncertain because of the relatively poor spatial cross-correlation of the data. The situation is further complicated by the fact that some of the pressure transducers located along the combustion chamber may be unable to effectively detect those modes whose pressure nodes fall nearby.
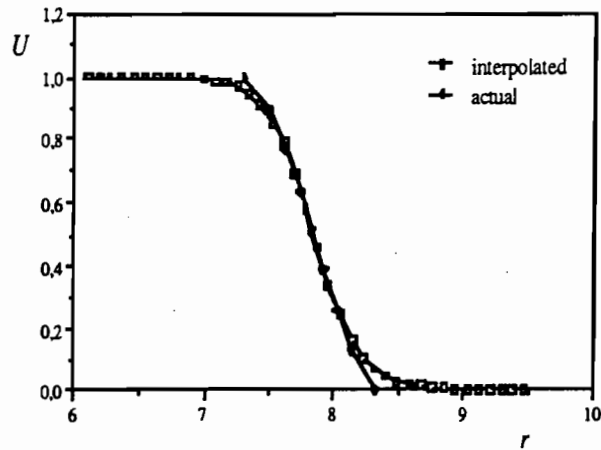

Figure 6. Typical normalized profile of the axial velocity in the shear layer for the LP3 motor.
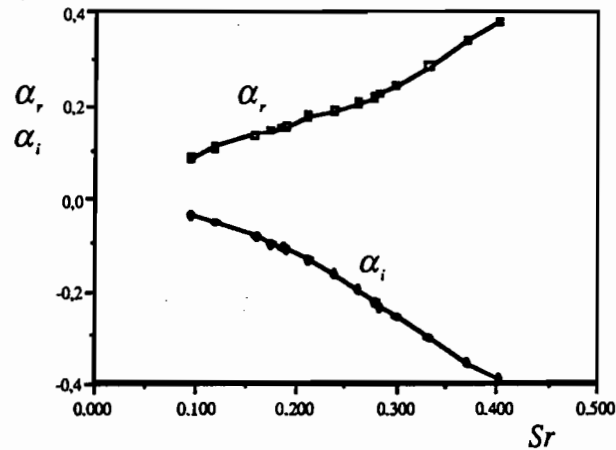

Figure 7. Complex wave number α as a function of the Strouhal number $Sr = \omega\delta/\Delta U$ for the LP3 motor at 26.6% web thickness burnt and $\bar{p} = 5.134$ MPa
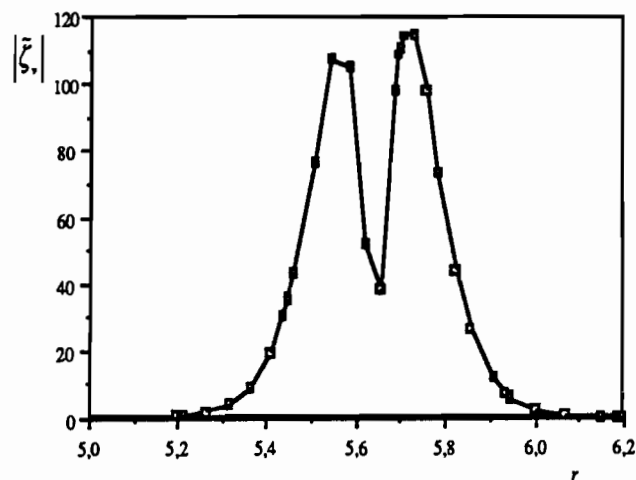

Figure 8. Modulus of the complex amplitude of the perturbation vorticity $\left|\tilde{\zeta}_v\right|$ v/s the radial coordinate r for the LP3 motor at 26.6% web thickness burnt and $\bar{p} = 5.134$ MPa
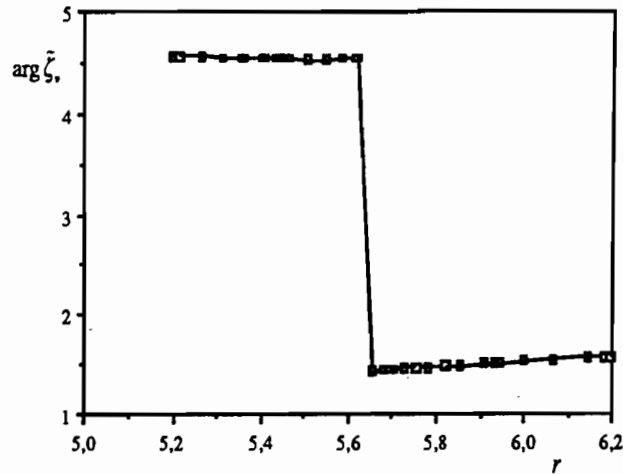
Figure 9. Argument of the complex amplitude of the perturbation vorticity $\arg \tilde{\zeta}_\nu$ v/s the radial coordinate r for the LP3 motor at 26.6% web thickness burnt and $\bar{p} = 5.134$ MPa

Table 5. Results of linear stability analysis. LP3 motor, 26.6% web combustion.

mode	f [Hz]	C_{β_ν}	predicted	observed
1L	361.7	0.113	unstable	stable
2L	731.2	0.204	unstable	unstable
3L	1019.1	0.326	unstable	unstable
4L	1393.8	0.504	unstable	unstable

Table 6. Results of linear stability analysis. LP3 motor, 75% web combustion.

mode	f [Hz]	C_{β_ν}	predicted	observed
1L	361.7	0.08	unstable	stable
2L	731.2	0.33	unstable	unstable
3L	1019.1	-0.13	stable	stable
4L	1393.8	-0.06	stable	stable

The criterion adopted here for stability discrimination consisted in considering the mode unstable when at least one transducer shows clear evidence of significant pressure oscillations at the relevant frequency.

Experimental data for the first combustion time (26.6% web thickness burnt) confirm numerical results except, perhaps, for the first mode, whose small value of the coefficient C_{β_ν} indicates, anyway, a weak driving. As for the fourth mode, contrary to the other cases, the experimental results are relatively uncertain since just one pressure transducer (placed between the second and third intersegment) indicates the presence of oscillations. Results relative to the second combustion time (75% web thickness burnt) are again in good agreement with experimental data: the third and fourth mode, predicted unstable at 25%, are now stable; furthermore, the second mode remains unstable. On the other hand, the first mode is predicted unstable, contrary to experimental data.
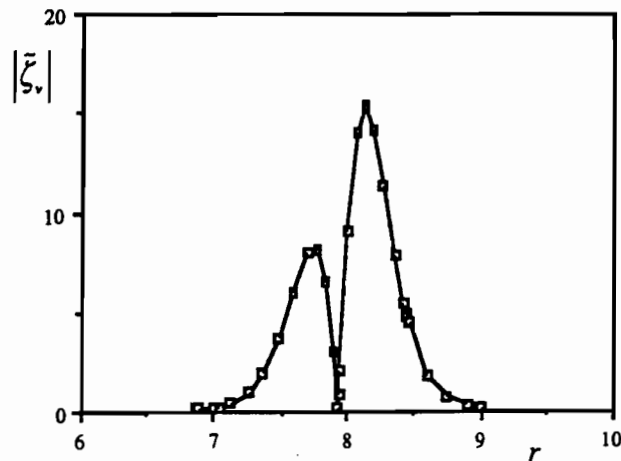

Figure 10. Modulus of the complex amplitude of the perturbation vorticity $\left|\tilde{\zeta}_\nu\right|$ v/s the radial co-ordinate r for the full-scale Ariane 5 P230 motor at 25% web thickness burnt and $\bar{p} = 4.63$ MPa

759

For the full-scale Ariane 5 P230 boosters the results of the stability analysis of the first three longitudinal modes in the combustion chamber under the excitation provided by the vortical wake from the inhibitor have been derived for three web thickness combustion times (25%, 50% and 75%). The frequencies of the first three longitudinal modes, corrected according to Culick's theory, are reported in Table 7, together with the corresponding wave numbers obtained from the shear layer stability analysis. Typical behaviors of the amplitude and phase of the perturbation vorticity in the shear layer of the inhibitor are plotted in Figure 10 and 11, respectively. The results of the stability analysis of the first three longitudinal modes in the combustion chamber under the excitation provided by the vortical wake of the inhibitor are summarized in Table 8 for the three combustion times under consideration. No experimental data are available for comparison. The first mode is predicted unstable for all burn times, although the coefficient C_β assumes rather small values. On the contrary, modes 2L and 3L are always predicted stable.
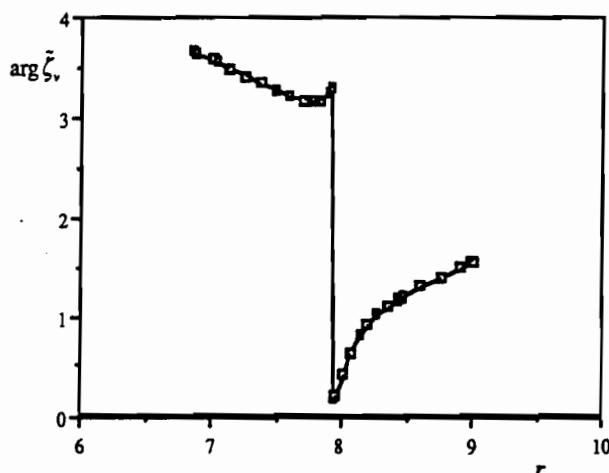

Figure 11. Argument of the complex amplitude of the perturbation vorticity $\arg \tilde{\zeta}_v$ as a function of the radial coordinate r for the full-scale Ariane 5 P230 motor at 25% web thickness burnt and $\bar{p} = 4.63$ MPa

Table 7. Modal frequencies and wave numbers.
P230 boosters, 25%, 50% and 75% web combustion.

| | | 25% | | | 50% | | | 75% | |
mode	f [Hz]	α_r	α_i	f [Hz]	α_r	α_i	f [Hz]	α_r	α_i
1L	18.3	0.29	-0.22	20.9	0.15	-0.15	22.7	1.04	-0.63
2L	37.3	1.08	-0.68	41.7	0.47	-0.43	44.6	2.34	-0.23
3L	59.7	2.11	-0.50	64.2	0.98	-0.67	67.1	----	----

Table 8. Results of linear stability analysis.
P230 boosters, 25%, 50%, and 75% web combustion

| web: | 25% | | 50% | | 75% | |
mode	C_β		C_β		C_β	
1L	0.07	unstable	0.003	unstable	0.011	unstable
2L	-0.05	stable	-0.105	stable	-0.083	stable
3L	-0.06	stable	-0.021	stable	--(*)	stable

(*) Here $\alpha_i > 0$, the shear layer remains stable, and there is no coupling with the acoustic field.

4. Conclusions

A number of concluding remarks can be drawn from the application of the present model to a realistic case and comparison with the corresponding experimental data:

- The predicted vortex-induced amplification/damping rates of longitudinal oscillations in the combustion chamber are much larger than the contributions of the other effects like pressure and velocity coupling, suspended particles, and grain motions, thereby indicating that the vortices shedding from the inhibitors are likely to be the major destabilizing factor in segmented solid propellant rockets. This conclusion is fully consistent with experience.
- The results refer to a rather idealized flow geometry, and are quite sensitive to the input data, especially the velocity profiles of the shear layer and the distance of the downstream surface from the inhibitor.
- Despite these limitations and the relatively uncertain interpretation of the available empirical data due to poor spatial cross-correlation, the results of the stability analysis are in surprisingly good agreement with the experiments. It seems, therefore, that the model is capable to correctly represent the behavior of the flow in the combustion chamber at least in an average sense, i.e. for times significantly longer than the typical oscillation period, even though the real instantaneous flow is probably far more complex than assumed.
- Within the obvious limitations inherent to the linearized approximation, the present model provides a rather general and efficient approach to the problem of rocket flow instabilities induced by vortical wakes, with the inclusion of the effects of all of the other major destabilizing factors. When properly applied, it represents a useful means for design analysis of segmented solid propellant rockets.

Acknowledgments

Nomenclature

a	sound speed, burning rate constant	M_b	Mach number at the burning grain
A	port cross-sectional area	n	burning rate exponent
A_b	combustion surface acoustic admittance	n	unit normal vector
A_n	nozzle acoustic admittance	p	pressure
c_p	specific heat at constant pressure	P	Helmholtz 's pressure mode shape
c^*	propellant characteristic velocity	r	radial coordinate
C_{β_v}	amplification/damping coefficient	R_o	inhibitor radial coordinate
i	imaginary unit	S	downstream boundary surface
g, h	functions	Sr	Strouhal number
k	corrected acoustic wave number	t	time
$I_0(z)$	modified Bessel function of the 1st kind	u	axial velocity component
K	Helmholtz acoustic wave number	v	radial velocity component
$K_0(z)$	modified Bessel function of the 2nd kind	U	shear layer axial velocity
l	acoustic mode index	ΔU	axial velocity difference across shear layer
ℓ	stand-off distance	V	combustion chamber volume
L	combustion chamber length	x	axial coordinate from shear layer origin
m_b	combustion mass flux	y	transversal coordinate in 2-D shear layers
M_c	Mach number in the combustion chamber	X	axial coordinate from motor head-end
M_e	chamber exit Mach number		

Greek Symbols

α	vortical wave number
α_r, α_i	vortical wave number real and imaginary parts
β_v	vortex-induced amplification/damping rate

Subscripts

a	acoustic
v	vortical

δ	shear layer thickness	
γ	specific heat ratio	
ζ	perturbation vorticity	
ϑ	circumpherential cylindrical coordinate	
ρ	propellant gas density	
ρ_p	propellant grain density	
ω	acoustic angular frequency	
ω_r, ω_i	acoustic frequency real and imaginary parts	
Ω	shear layer unperturbed vorticity	

Special Notations

q'	perturbation quantity, differentiation
$\tilde{q}$	complex amplitude of perturbation
$\bar{q}$	space average
$\langle q \rangle$	time average

Bibliography

Betchov R. and Criminale W.O. Jr., 1967, "Stability of Parallel Flows", *Academic Press*, New York.

Brown R.S., *et al.*, 1981, "Vortex Shedding as a Source of Acoustic Energy in Segmented Solid Rockets", *J. of Spacecraft and Rockets*, Vol. 18, No. 4, pp. 312-319.

Culick F.E.C., 1970, "Stability of Longitudinal Oscillations with Pressure and Velocity Coupling in a Solid Propellant Rocket", *Combustion Science and Technology*, Vol. 2, pp. 179-201.

Culick, F.E.C., 1973, "The Stability of One-Dimensional Motions in a Rocket Motor", *Combustion Science and Technology*, Vol. 7, pp. 165-175.

Culick, F.E.C., 1975, "Stability of Three-Dimensional Motions in a Combustion Chamber", *Combustion Science and Technology*, Vol. 10, pp. 109-124.

Culick, F.E.C., 1990, "Some Recent Results for Nonlinear Acoustics in Combustion Chambers", *AIAA Paper No. 90-3927, AIAA 13-th Aeroacoustic Conf.*, Tallahassee, Florida, USA.

Flandro G.A., 1986, "Vortex Driving Mechanism in Oscillatory Rocket Flows", *J. of Propulsion and Power*, Vol. 2, N° 3, May-June 1986, pp. 206-217.

Kuentzmann P., 1991, "Instabilites de Combustion", *Combustion of Solid Propellants*, AGARD-LS-180, July 1991.

Michalke A., 1965, "On Spatially Growing Disturbances in an Inviscid Shear Layer", *J. Fluid Mechanics*, Vol. 23, part 3, pp. 521-544.

Stoer J. and Bulirsch R., 1976, "Introduzione all'Analisi Numerica", *Zanichelli*, Bologna, Italy.

Yang V., Kim S.I. and Culick, F.E.C., 1990, "Triggering of Longitudinal Pressure Oscillations in Combustion Chambers. I: Nonlinear Gasdynamics", *Combustion Science and Technology*, Vol. 72, pp. 183-214.

Vuillot F., *et al.*, 1993, "Experimental Validation of Stability Assessment Methods for Segmented Solid Propellant Motors", *AIAA Paper No. 93-1883, 29th Joint Propulsion Conf.*, Monterey, California, USA.

Sommario

Un modello lineare per l'analisi delle oscillazioni fluidodinamiche longitudinali nei razzi a propellente solido è stato sviluppato ed applicato ai boosters dell'Ariane 5. Le frequenze naturali sono corrette come proposto da Culick per tener conto degli effetti del flusso medio, dell'aggiunta di massa dal grano, dell'accoppiamento con il campo di pressione, dell'ammettenza dell'ugello, e della geometria interna della camera di combustione. Nei motori a propellente solido segmentato la fonte principale di eccitazione di oscillazioni acustiche è spesso costituita dall'accoppiamento tra i vortici rilasciati dagli inibitori agli intersegmenti ed il campo acustico nella camera di combustione. Tale accoppiamento è analizzato mediante il modello di Flandro, che fornisce il contributo indotto dalla scia vorticosa all'amplificazione o smorzamento delle oscillazioni acustiche. Le frequenze acustiche lineari sono considerate come dati d'ingresso per lo sviluppo dei vortici nella scia, che è descritto mediante la classica teoria lineare di stabilità dei flussi paralleli. La valutazione del rischio di instabilità fluidodinamiche indotte dalla presenza di vortici è stata effettuata per i principali modi a vari tempi di combustione per una configurazione in scala ridotta e per il prototipo. Le previsioni del modello sono in buon accordo con i risultati sperimentali disponibili per la configurazione in scala.

AIDAA

ASSOCIAZIONE ITALIANA DI AERONAUTICA E ASTRONAUTICA

ATTI DEL XII CONGRESSO NAZIONALE

Como 20-23 luglio 1993
Villa Olmo

VOLUME I